Resonance Raman Study of Cyanide-Ligated Horseradish Peroxidase. Detection of Two Binding Geometries and Direct Evidence for the "Push–Pull" Effect†

Jamil Al-Mustafa and James R. Kincaid*

Chemistry Department, Marquette University, Milwaukee, Wisconsin 53233

Received September 17, 1993; Revised Manuscript Received December 8, 1993®

ABSTRACT: Resonance Raman spectroscopy has been employed to investigate the structure of cyanide adducts of the basic isoenzymes of horseradish peroxidase (HRP) in the pH range 5.5–12.5. Evidence for the binding of cyanide in two forms, characterized by the reversal of ordering of the Fe–CN stretching and Fe–C–N bending vibrations, is observed. Moreover, it is shown that both conformers exhibit an acid–alkaline transition in the pH range employed. In the first conformer, the Fe–C–N linkage is essentially linear, exhibiting axial Fe–CN stretching and Fe–C–N bending frequencies at 453 and 405 cm^{-1}, respectively (at pH 5.5) (Lopez-Garriga et al., 1990). In the second conformer, the Fe–C–N fragment is bent, and the axial stretching and bending modes have been identified at 360 and 422 cm^{-1} at pH 5.5. At pH 12.5, the ν[Fe–CN] stretching mode of the linear conformer shifts down by 9 cm^{-1} to 444 cm^{-1} while the bending frequency remains unchanged. For the bent conformer at this pH, the stretching mode shifts to 355 cm^{-1} (−5 cm^{-1}), and the bending vibration shifts slightly to lower frequency by 2 cm^{-1} to 420 cm^{-1}. The observed pH-dependent shift of the ν[Fe–CN] stretching mode of the linear conformer is attributed to the direct effect of deprotonation of a distal-side amino acid residue while the shift of ν[Fe–CN] of the bent conformer is most reasonably ascribable to indirect alteration of the iron–proximal histidine linkage induced by the distal-side deprotonation, a spectral response which reflects a protein-coupled "push–pull" mechanism for heterolytic O–O bond cleavage.

Horseradish peroxidase (HRP) (donor H_2O_2 oxidoreductase, EC 1.11.1.7) catalyzes the oxidation of various substrates by hydrogen peroxide as its specific oxidant. Like hemoglobin subunits, myoglobin, and cytochrome *c* peroxidase, HRP contains a noncovalently bonded iron protoporphyrin IX coordinated to a proximal histidine residue and resides in a cavity formed by a single polypeptide chain. The structural differences in the folded polypeptide chain in the vicinity of the heme cofactor dictate the biological function of these proteins. Unlike hemoglobin and myoglobin which are biologically active in their ferrous state and bind O_2 reversibly, HRP is biologically active in its ferric state and binds dioxygen irreversibly in the ferrous state. Study of the structural differences in the proximal and distal pockets of heme proteins is vital for elucidating the factors which facilitate the activation of H_2O_2 and the rupture of the O–O bond in the catalytic cycle. The heme active sites of cytochrome *c* peroxidase and HRP contain a proximal histidine with a strongly hydrogen-bonded N_δ proton and a distal histidine and arginine, amino acids residues known to be capable of participating in hydrogen-bonding interaction with the natural substrate H_2O_2 (Finzel, 1984; Sakurada, 1986; Thanabal, 1987). It has been suggested (Finzel, 1984; Poulos, 1987; Thanabal, 1988; Dawson, 1988; Dunford, 1991) that these active-site structural features promote the heterolytic O–O bond cleavage of hydrogen peroxide and the formation of the reactive intermediate through the so-called "push–pull" mechanism. In the last few years, considerable effort has been devoted to the investigation of these structural differences by various techniques including NMR (La Mar, 1980, 1989), EPR (Palmer, 1979), EXAFS (Chance, 1984), and resonance Raman (RR) spectroscopy (Spiro, 1988; Han, 1989). These studies were conducted not only on the native forms but also on genetically engineered mutants (Morikis, 1989) and on adducts of these proteins with various exogenous ligands (e.g., F^-, CN^-, CO, and NO).

Yamazaki et al. (1978) proposed that heme-linked ionization plays an important role in the catalytic activity of HRP and suggested the distal histidine to be the specific ionizing group. Teraoka et al. (1981) found that the deprotonation of the distal histidine in ferrous HRP leads to the weakening of the iron–proximal histidine linkage, Fe–N_ϵ, concluding that the effect is communicated to the proximal side through the strongly hydrogen-bonded proton at the N_δ position of the proximal histidine. Later Battacharyya et al. (1992) reported that the chemical derivatization of the distal histidine leads to the inactivation of HRP, confirming an essential role for this residue in the catalytic cycle of HRP.

Addition of CN^- to the native isoenzymes of HRP leads to the formation of low-spin, cyanide-bound HRP. Cyanoferric HRP has been reported to undergo an acid–alkaline transition at pH 10.6 (for isoenzymes B and C) with the CN^- being retained (Morishima, 1977; de Ropp, 1984). The binding of CN^- to HRP was reported (Thanabal, 1988) to occur in concert with uptake of a proton that binds to distal His-42, generating an imidazolium ion that forms a strong hydrogen bond with bound cyanide in the pH range 4–11. Yoshikawa et al. (1985) studied the C–N stretching modes of the bound cyanide in both the ferric and ferrous derivatives of HRP by IR spectroscopy and reported the observation of complex band shapes that can be deconvoluted into at least two simple Gaussian curves. The authors suggested the possibility of variations in the binding geometry of cyanide to HRP. Lopez-Garriga et al. (1990) studied the cyanide adducts of both HRP and myeloperoxidase (MPO) by RR spectroscopy and concluded that the Fe–CN linkage is bent in MPO but is linear in HRP and attributed the difference in behavior to a more constrained pocket in myeloperoxidase. A downshift of

† This work was supported by a grant from the National Institutes of Health (DK35153).

® Abstract published in *Advance ACS Abstracts,* February 1, 1994.

0006-2960/94/0433-2191$04.50/0

5 cm^{-1} in the Fe–CN stretching mode upon raising the pH from 7.4 to 10.6 was detected for MPO while HRP was reported to not exhibit a significant shift in this pH range.

RR spectroscopy has been shown to be a powerful technique for the investigation of ligand bonding and geometry and for elucidating the effect of the distal- and proximal-side steric and electronic interactions on the disposition of the axial ligands (Yu, 1988). However, a recent report of RR studies of cyanide-ligated HRP is inconsistent with the results obtained by IR and NMR, in the sense that no evidence for multiple conformers and hydrogen bonding was observed in the RR study. We also have reinvestigated (Lopez-Garriga et al., 1990) the RR spectra of the cyanide adduct of HRP and herein report, for the first time, the detection of a second form of ferric HRP–CN and document the observation of pH-dependent downshifts in the frequencies of the axial modes of both forms.

EXPERIMENTAL PROCEDURES

Materials and Methods. Horseradish peroxidase (HRP) type II was purchased from Sigma (St. Louis, MO) as lyophilized, salt-free powder. Potassium cyanide was purchased from Aldrich Chemical Co. (Milwaukee, WI). $K^{13}C^{14}N$, $K^{12}C^{15}N$, and $K^{13}C^{15}N$, at 99% enrichment, were obtained from Isotech Inc. (Miamisburg, OH). HRP was purified by the method of Shannon et al. (1966), and the different isoenzymes were identified on the basis of their chromatographic mobility. HRP was dissolved in small volume of 5 mM acetate buffer (pH 4.5) and loaded onto a CM-52 (Whatman) column (2 × 25 cm) equilibrated with the same buffer. The acidic isoenzymes were completely eluted, and the column was further washed with about 100 mL of the same buffer. Isoenzymes B and C were separated from isoenzymes D and E by employing a linear gradient consisting of 500 mL of 5 mM acetate buffer (pH 4.5) and 500 mL of 100 mM acetate buffer (pH 4.5). Isoenzyme B elutes first, followed by isoenzyme C. The fractions containing pure isoenzymes B or C were collected and pooled. For the preparations that contain the four basic isoenzymes, a linear gradient consisting of 500 mL of 5 mM acetate buffer (pH 4.5) and 500 mL of 500 mM acetate buffer (pH 4.5) was used. The buffer exchange was achieved by chromatographing the HRP solution over a Sephadex G-25 (Pharmacia) column equilibrated with the desired buffer. The purified enzyme was dissolved either in 250 mM acetate buffer (pH 5.5), in 250 mM phosphate buffer (pH 7.0), or in 250 mM carbonate buffer (pH 10.5 or 11.6). The enzyme concentration was measured assuming ϵ = 103 mM^{-1} cm^{-1} at 403 nm, and only the fractions with a purity index, R_z (i.e., A_{403}/A_{280}), greater than 3.2 were used (Shanon, 1966).

Cyanoferric HRP complexes were prepared either by the addition of a small amount of solid potassium cyanide (or its isotopic form) to 0.2 mL of 0.1 mM HRP in a 5-mm NMR tube or by the addition of a buffered solution of potassium cyanide to the HRP solution to a final concentration of 50 mM cyanide. No significant differences in the RR spectra were osberved for the two methods.

Spectroscopic Measurements. The RR spectra were acquired either with a Spex 1403 double monochromator equipped with a Spex DM1B data station and Hamamatsu R-928 photomultiplier tube or with a Spex 1269 spectrometer equipped with a Princeton Instrument ICCD-576 UV-enhanced dectector and a 413.1-nm notch filter (Kaiser Optical Systems, Inc., Ann Arbor, MI). The 413.1-nm line was from a Coherent Innova Model 100-K3. The NMR tube containing the solution was spun during illumination to avoid local heating. The accumulation time for the spectra obtained with the 1269 spectrometer was 800 s, and the laser power used was 15 mW. The spectra obtained with the 1403 system are the summation of 10 scans, with a laser power of 25 mW.

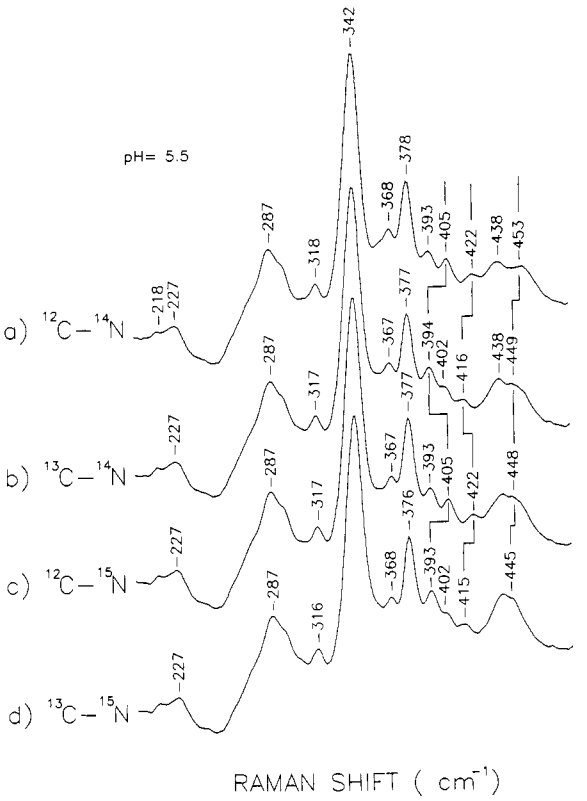

FIGURE 1: Resonance Raman spectra of the isotopically labeled cyanide adducts of isoenzyme B of HRP at pH 5.5 in 250 mM acetate buffer. The enzyme concentration was 0.1 mM, and the KCN concentration was 50 mM. Excitation line, 413.1 nm; laser power at the sample, 15 mW. Spectra were obtained with a 1269 Spex single monochromator equipped with a Princeton Instrument ICCD detector. Collection time was 10 min.

RESULTS

Cyanide Adducts of the Basic Isoenzymes of HRP. Figure 1 shows the low-frequency RR spectra of the cyanide adducts of horseradish peroxidase isoenzyme C (HRP-C) with the different isotopomers of potassium cyanide obtained with 413.1-nm excitation at pH 5.5. Comparison of the spectra reveals three isotope-sensitive modes. Two of these modes, those at 453 and 405 cm^{-1} (Figure 1a), have been previously reported (Lopez-Garriga et al., 1990). The third mode at 422 cm^{-1} is here reported for the first time. The 454-cm^{-1} mode exhibits a monotonic isotope shift irrespective of the position of labeling as the total mass of the cyanide ion increases, shifting to 449 cm^{-1} ($^{13}C^{14}N^-$), 448 cm^{-1} ($^{12}C^{15}N^-$), and 445 cm^{-1} ($^{13}C^{15}N^-$). This isotope dependence is similar to the behavior of the mode identified (Yu, 1984) at 453 cm^{-1} in cyanomet CTT III and assigned to the ν[Fe–CN] stretching vibration in ferric HRP–CN (Lopez-Garriga et al., 1990).

The line at 405 cm^{-1} appears to be composed of two overlapping components: an isotope-sensitive component that can be seen in the spectra of the $^{12}C^{14}N^-$ and $^{12}C^{15}N^-$ adducts (Figure 1a,c). This component shifts to 393 cm^{-1} in the spectra of the $^{13}C^{14}N^-$ and $^{13}C^{15}N^-$ adducts (Figure 1b,d). This type of decrease–increase–decrease (i.e., zigzag) isotope dependence is characteristic of the δ[Fe–C–N] bending mode (Yu, 1984). Accordingly, we assign the isotope-sensitive component at

405 cm^{-1} to the δ[Fe–C–N] bending vibration in HRP. The second, isotope-insensitive, component can be seen as the residual feature at 402 cm^{-1} in the spectra of $^{13}C^{14}N^-$ and $^{13}C^{15}N^-$ complexes (Figure 1b,d).

The third isotope-sensitive mode (422 cm^{-1}) is newly identified in this report. This line also exhibits a zigzag isotope shift pattern, occurring at 422 cm^{-1} ($^{12}C^{14}N^-$), 416 cm^{-1} ($^{13}C^{14}N^-$), 422 cm^{-1} ($^{12}C^{15}N^-$), and 415 cm^{-1} ($^{13}C^{15}N^-$). On the basis of this pattern, we assign this mode to the δ[Fe–C–N] bending vibration of the second conformer of cyanoferric HRP.

In addition to the isotope-sensitive modes mentioned above, we were able to identify a number of porphyrin modes that exhibit a small but a definite isotope dependence that can be attributed to vibrational coupling of the porphyrin modes with axial ligand modes; e.g., the modes at 378, 368, and 318 cm^{-1} exhibit 2-cm^{-1} downshifts upon the substitution of $^{13}C^{15}N^-$ (Figure 1d) for $^{12}C^{14}N^-$ (Figure 1a). These modes fall in the region where out-of-plane modes are observed, and the resulting shifts can be brought by coupling to the Fe–C–N vibrations which are also out-of-plane in nature.

A closer examination of the region between the porphyrin modes at 368 cm^{-1} and the strong mode at 344 cm^{-1} (ν_8) reveals the presence of an isotope-sensitive intensity fluctuation. This is the region where the ν[Fe–C] stretching vibrations of the cyanide adducts of myeloperoxidase (Lopez-Garriga et al., 1990), lactoperoxidase (Hu, 1993), and one form of sulfite reductase (Han, 1989) have been identified. In order to locate the stretching mode associated with the second structural form of HRP–CN, we have carefully analyzed computer-generated difference spectra of the various isotopomeric forms in search of a feature which exhibits a monotonically decreasing isotopic shift pattern. Figure 2 shows the difference spectra obtained by subtraction of pairs of the various spectra seen in Figure 1. The upper trace shows the difference spectrum obtained by subtraction of the spectrum of $^{13}C^{15}N^-$ (Figure 1d) from that of the $^{12}C^{14}N^-$ adduct (Figure 1a). In addition to the three isotope-sensitive modes at 453, 422, and 405 cm^{-1} identified before, this trace reveals a fourth isotope-sensitive feature in the region between 365 and 353 cm^{-1}. The second and third traces show difference spectra obtained by subtraction of pairs of the spectra of adducts in which the mass of the carbon atoms is equal but the total mass of the cyanide isotopomers is different. In these two cases, the bending vibrations should occur at the same frequency and thus cancel out, while features associated with the stretching modes should appear in the difference spectra. The second trace shows the results of subtracting the spectrum of the $^{12}C^{15}N^-$ adduct (Figure 1c) from that of the $^{12}C^{14}N^-$ adduct (Figure 1a). This trace reveals intensity variations in two regions. The variation near 450 cm^{-1} is ascribed to the stretching mode that has been identified at 454 cm^{-1}. The difference feature identified at 365 and 356 cm^{-1} reveals the existence of a second isotope-sensitive band in this region. The appearance of this mode in the third trace, obtained by subtraction of the spectrum of the $^{13}C^{15}N^-$ adduct (Figure 1d) from the spectrum of the $^{13}C^{14}N^-$ adduct (Figure 1b), along with observation of its complete cancelation in the fourth trace, obtained by subtraction of the spectrum of the $^{13}C^{14}N^-$ adduct (Figure 1b) from that of the $^{12}C^{15}N^-$ (Figure 1c) adduct, leaves no doubt that this mode exhibits a monotonic downshift with the increase of the total mass of the cyanide. From the small shoulder on the low-frequency side of the 368-cm^{-1} porphyrin mode (see the upper trace in Figure 4 also), we estimate that the mode responsible for the intensity fluctuation in this region occurs

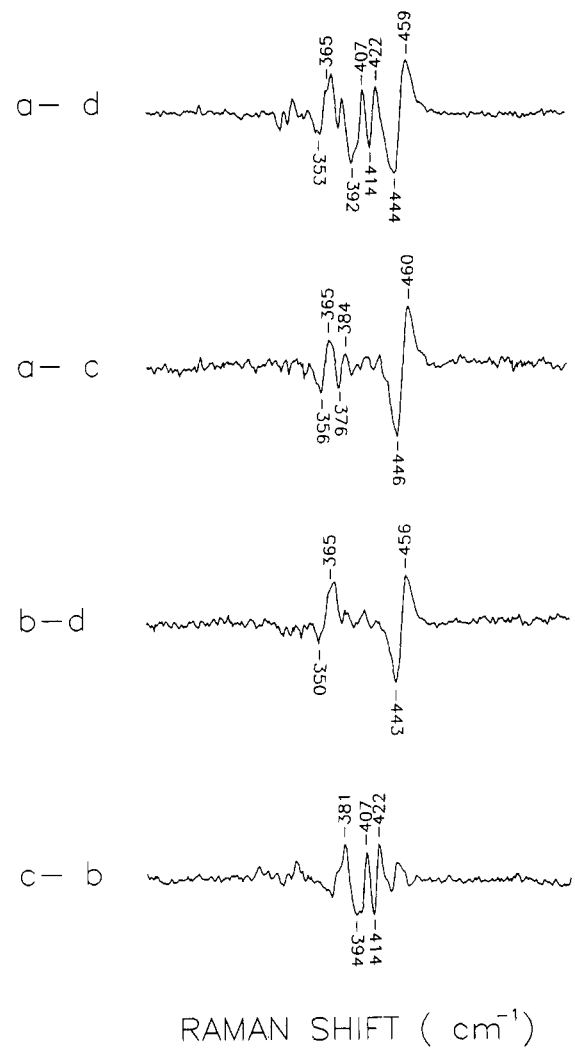

FIGURE 2: Computer-generated difference spectra obtained by subtraction of the various pairs of spectra in Figure 1.

near 360 cm^{-1}. This frequency is virtually identical to those of the ν[Fe–CN] stretching frequencies identified for myeloperoxidase (361 cm^{-1}) (Lopez-Garriga et al., 1990) and lactoperoxidase (360 cm^{-1}) (Hu, 1993), and is comparable to one of the stretching frequencies identified in *Escherichia coli* sulfite reductase hemoprotein (353 cm^{-1}) (Han, 1989). Accordingly, we assign the feature at 360 cm^{-1} to the ν[Fe–CN] stretching vibration of the newly identified form of the HRP–cyanide adduct. The difference feature near 380 cm^{-1} in the second and fourth traces of Figure 2 is due the small shift observed in the 378-cm^{-1} feature mentioned earlier.

RR measurement of the cyanide adducts of preparations that contain pure isoenzyme B (spectra are not shown) or a mixture of the basic isoenzymes B, C, D, and E yields spectra which are virtually indistinguishable from those obtained for isoenzyme C.

IR measurement on cyanoferrous HRP in H_2O and D_2O (Yoshikawa, 1985) revealed that the cyanide moiety in this derivative is hydrogen-bonded. An NMR pH titration in the pH range 3–11.4 also revealed that the cyanide-bound ferric HRP undergoes an alkaline transition to a new form at pH 10.6 (Morishima, 1977; de Ropp, 1984; Thanabal, 1988). In order to characterize the alkaline form of cyanoferric HRP, we measured the RR spectra of the natural-abundance cyanide adduct of HRP as a function of pH in the range 5.5–12.5 as shown in Figure 3. As the pH is raised, the intensity of the mode at 453 cm^{-1} in the RR spectrum of cyanoferric HRP

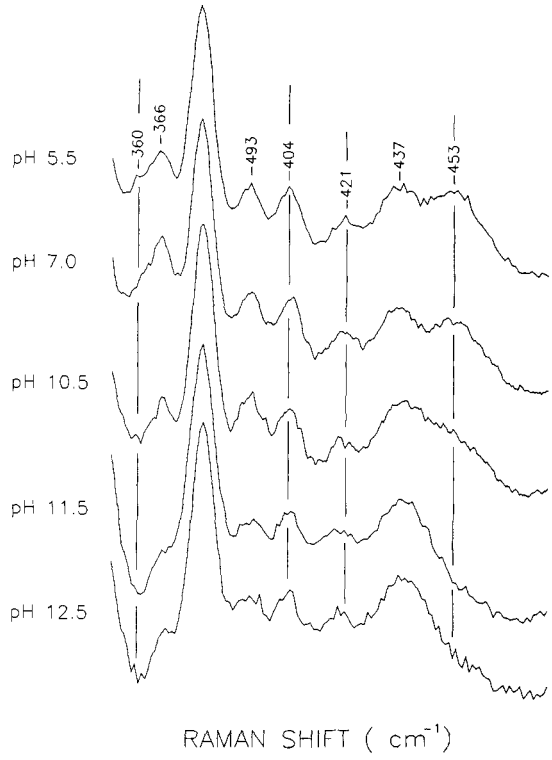

FIGURE 3: Resonance Raman spectra of the natural-abundance cyanide adducts of the basic isoenzymes of HRP in the pH range 5.5–12.5. The rest of the experimental conditions are as in Figure 1 except the spectra were obtained with a 1403 Spex double monochromator.

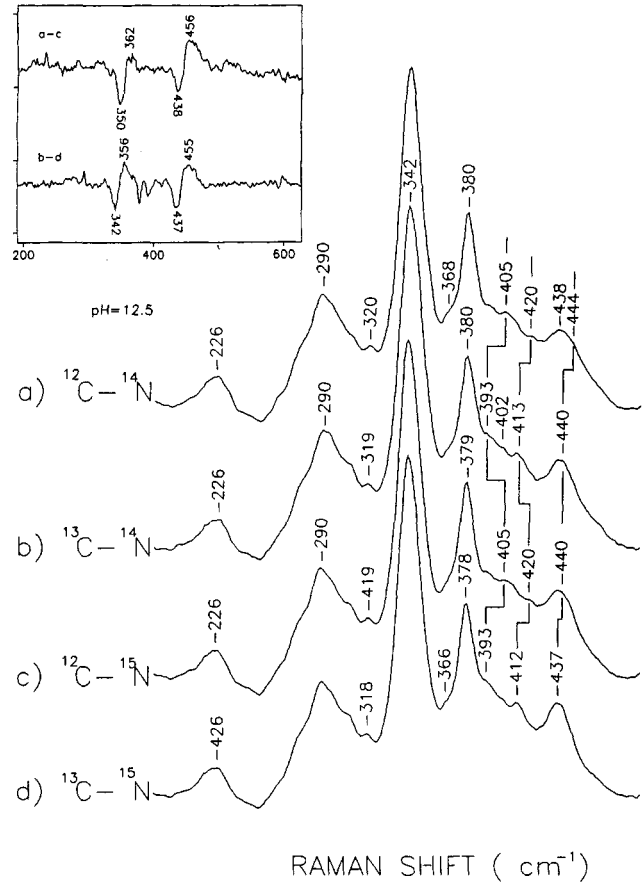

FIGURE 4: Resonance Raman spectra of the cyanide adducts of the basic isoenzymes at pH 12.5 in 250 mM carbonate buffer. The rest of the experimental conditions are as in Figure 1. The inset shows difference spectra obtained by subtraction of trace c from trace a (upper trace) and of trace d from trace b (bottom trace).

at pH 5.5 (top trace) decreases with a concomitant increase in intensity in the region between 435 and 438 cm^{-1}. At pH 12.5 (bottom trace), the mode at 453 cm^{-1} disappears completely and is replaced by a new isotope-sensitive mode that is severely overlapped with the porphyrin mode at 438 cm^{-1}. Although the exact frequency of the new mode is difficult to determine, we estimate it to be at about 444 cm^{-1}. As shown in Figure 4, this mode exhibits a monotonic shift pattern to 440 cm^{-1} ($^{13}C^{14}N$, $^{12}C^{15}N^-$) and finally to 437 cm^{-1} ($^{13}C^{15}N^-$). We assign this mode to the ν[Fe–CN] stretching vibration in the alkaline form of the first conformer.

The RR spectra of the cyanide-bound HRP at alkaline pH also reveal two isotope-sensitive modes that exhibit zigzag isotope shift patterns. The isotope-sensitive mode observed at 405 cm^{-1} (at pH 5.5) does not show any measurable shift upon transition from the acidic to the alkaline form (Figures 3 and 4). Thus, as is shown in Figure 4, this mode occurs at 405 cm^{-1} ($^{12}C^{14}N^-$), 393 cm^{-1} ($^{13}C^{14}N^-$), 405 cm^{-1} ($^{12}C^{15}N^-$), and 493 cm^{-1} ($^{13}C^{15}N^-$). The isotope-sensitive mode observed at 422 cm^{-1} in the RR spectrum of the acidic form of cyanoferric HRP (at pH 5.5) shows a small but a definite downshift (2 cm^{-1}) upon transition from the acidic to the alkaline form. In the alkaline form, as shown in Figure 4, this mode is observed at 420 cm^{-1} and shifts to 413 cm^{-1} ($^{13}C^{14}N^-$), 419 cm^{-1} ($^{12}C^{14}N^-$), and 413 cm^{-1} ($^{13}C^{15}N^-$). We assign the modes at 405 and 420 cm^{-1} to δ[Fe–C–N] bending vibrations of the first and second conformers of the cyanide adduct in the alkaline forms.

It was difficult to determine the exact frequency of the mode assigned for the ν[Fe–CN] stretching vibration in the alkaline form of the second conformer, because it is hidden by the intense ν_8 porphyrin mode at 344 cm^{-1}. Figure 3 shows the RR spectra of the natural-abundance cyanide adduct of basic isoenzymes of HRP at different pH values. In addition to the disappearance of the mode at 453 cm^{-1} and the small shift in the bending mode observed at 422 cm^{-1}, it reveals a subtle decrease in intensity at 360 cm^{-1}. The pronounced shoulder observed at 360 cm^{-1} at pH 5.5, assigned to the [Fe–CN] stretching vibration of the acidic form of the second conformer, disappears and is replaced by a deep trough at pH 12.6. Concomitantly, a new shoulder appears to be forming at 355 cm^{-1}. The insert in Figure 4 shows two difference spectra obtained by subtraction of the spectrum of the $^{12}C^{15}N^-$ adduct from that of the $^{12}C^{14}N^-$ adduct (top trace) and by subtraction of the spectrum of the $^{13}C^{15}N^-$ adduct from that of the $^{13}C^{14}N^-$ adduct. Both traces reveal the presence of two stretching modes: one near 440 cm^{-1} that is ascribed to the stretching mode of the alkaline form mentioned above and another mode near 350 cm^{-1} that we assign to the ν[Fe–CN] stretching vibration of the alkaline form of the second conformer. We estimate that this mode shifts from 360 cm^{-1} in the acidic form to 355 cm^{-1} in the alkaline form. The magnitude of this shift (–5 cm^{-1}) is identical to the pH-induced shift observed for myeloperoxidase (Lopez-Garriga et al., 1990) and lactoperoxidase (Hu, 1993). Similar behavior was observed for the acidic isoenzymes of HRP (spectra not shown). The frequencies of the Fe–C–N axial modes are summarized in Table 1.

DISCUSSION

Structural Heterogeneity and the Acid–Alkaline Transition. (1) Spectral Behavior. As was shown in the previous sections, the RR results presented here provide unambiguous evidence that the cyanide ligand binds in two distinct

Table 1: Axial Mode Frequencies (cm^{-1}) for Cyanoferric HRP with Different Labeled Cyanide Isotopomers

species	pH	mode	isotope $^{12}C^{14}N^-$	$^{13}C^{14}N^-$	$^{12}C^{15}N^-$	$^{13}C^{15}N^-$
HRP–CN	5.5	ν	453	449	449	445
		δ	405	393	405	393
		ν	460			
		δ	422	416	421	415
	11.6	ν	444	439	440	435
		δ	405	393	405	339
		ν	355			
		δ	420	413	419	413

geometries, giving rise to two conformers. One conformer is essentially linear, exhibiting ν[Fe–CN] and δ[Fe–C–N] modes at 453 and 405 cm^{-1}, spectral behavior which is quite similar to that observed for several other heme proteins and model compounds known to form essentially linear Fe–C–N linkages (Yu, 1984, 1988; Han, 1989; Lopez-Garriga et al., 1990; Tanaka, 1987; Uno, 1988). The second conformer exhibits ν[Fe–CN] and δ[Fe–C–N] frequencies at 360 and 422 cm^{-1}, a pattern which is virtually identical to those of cyanoferric myeloperoxidase (Lopez-Garriga et al., 1990), lactoperoxidase (Hu, 1993), and one form of cyanoferric sulfite reductase (Han, 1989), this pattern being consistent with a bent Fe–C–N fragment.

Cyanoferric HRP has been studied in detail by proton and deuterium NMR (La Mar, 1980, 1989; de Ropp, 1984; Thanabal, 1987, 1988; Bancie, 1991). All of these studies failed to detect the heterogeneity in the CN^- adducts of ferric HRP. Also, Behere et al. (1985) studied cyanoferric HRP by ^{15}N-NMR and identified a single resonance assignable to the nitrogen atom of the bound cyanide anion. The failure to detect by NMR the two conformers identified in this report implies that the rate of interconversion of the two conformers is too great for the NMR time scale. The single resonance detected by ^{15}NMR must represent a time-weighted average of the two conformers. A similarly fast rate of conformer interconversion has been reported for the CO adducts of metmyoglobin (Caughey, 1981) while multiple ν[Fe–CO] and ν[C–O] modes are readily detected by vibrational spectroscopy (Caughey, 1981, 1983; Frauenfelder, 1991; Sage, 1991a,b).

It is especially interesting to note not only that both conformers persist at all pH values but also that they experience congruent frequency shifts upon raising the pH. Referring to Figures 2 and 4 (and the inset in Figure 4), it is seen that ν[Fe–CN] for the linear form shifts from 453 cm^{-1} (pH 5.5) to 444 cm^{-1} (pH 12.5) while ν[Fe–CN] shifts from ~360 cm^{-1} (pH 5.5) to ~355 cm^{-1} (pH 12.5) for the bent conformer. As will be shown below, the existence of two distinct spectral patterns and their similar response to increasing the pH of the solution are entirely consistent with the known active-site structure and the proposal that deprotonation of a single distal-side amino acid (His-42) induces changes in both distal- and proximal-side environments.

(*2*) *Structural Interpretation.* The crystal structure of the cyanide adduct of the closely related cytochrome *c* peroxidase reveals that the nitrogen atom of the bound cyanide is within hydrogen-bonding distance from three amino acid residues: Arg-48, Trp-51, and His-52 (Edwards, 1990). Only two of these amino acids (Arg-38 and His-42) are conserved and situated in similar positions in HRP, while the distal Trp-51 is replaced by Phe-41 (Sakurada, 1986; Thanabal, 1987). This distal-side active-site structure provides at least two polar residues which are capable of participating in a relatively strong hydrogen-bonding interaction with bound exogenous ligands, including cyanide. In fact, it is generally accepted that resting-state HRP and other peroxidases bind HCN to form the cyanoferric complex, the proton simultaneously protonating the distal histidine to form an imidazolium group which strongly hydrogen bonds to the bound cyanide ligand (Dunford, 1982; Edwards, 1990; Thanabal, 1988).

The relatively complicated RR pattern and response to pH changes reported here are reasonably explained on the basis of the above information. Thus, the bound cyanide may adopt one of two different conformations. The first, having an essentially linear geometry, is strongly hydrogen-bonded to the imidazolium group of the distal histidine (His-42), giving rise to the expected RR pattern (i.e., ν[Fe–CN] and δ[Fe–C–N] modes near 450 and 400 cm^{-1}, respectively). The second, apparently minor (based on its weaker RR intensity) conformer may hydrogen-bond to the arginine residue, which (being much further off-axis) induces a bent geometry with its characteristic RR spectral pattern (i.e., ν[Fe–CN] and δ[Fe–C–N] modes near 460 and 420 cm^{-1}, respectively).

The behavior of the RR spectral pattern for each conformer upon increasing the pH is also consistent with our current understanding of the response of the active site to changes in pH. Thus, it is known from recent NMR studies (Morishima, 1977; de Ropp, 1984; Thanabal, 1988) that the distal histidine hydrogen bond to the bound cyanide is stabilized by electrostatic forces and this residue remains protonated up to pH 11. As can be seen in Figures 2, 3, and 4, at pH values near and above 10, the 453-cm^{-1} features decreases in intensity, and a new band grows in near 444 cm^{-1}; i.e., upon deprotonation of the distal histidine, the hydrogen bond to the bound cyanide is lost which destabilizes the Fe–CN bond, giving rise to the 9-cm^{-1} shift to lower frequency.

While this shift to lower frequency upon the elimination of the hydrogen bond is as expected for the linear form, it is not immediately obvious why the ν[Fe–CN] associated with the second conformer should shift from 360 to 355 cm^{-1}. Clearly, the arginine residue remains protonated even at this high pH value since deprotonation would have eliminated the hydrogen bonding and abolished the second conformer. The RR data not only document the fact that the bent conformer persists but also indicate that the Fe–CN bond is weakened at this higher pH. This behavior can be reasonably interpreted as consequence of proximal-side changes, as discussed below.

It is well-known from RR studies of the ferrous form of HRP that deprotonation of the distal histidyl imidazole induces a corresponding weakening (albeit slight; 3–5 cm^{-1}) of the bond between the heme iron and the proximal imidazole. Interestingly, the opposite behavior was observed for the ferric state, ν[Fe–N_ϵ(His)] exhibiting a significant increase at high pH (Teraoka, 1981). Thus, the observed weakening of the Fe–CN bond can be reasonably attributed to a variation in the trans-proximal Fe–N_ϵ(His) bond strength upon the acid–alkaline transition. Vibrational analysis predicts that while a strictly linear Fe–C–N fragment is only slightly, if at all, sensitive to the trans iron–ligand bond, the bent form is expected to be more sensitive (Lopez-Garriga et al., 1990). The same vibrational analysis also predicts that strengthening of the trans Fe–N_ϵ(His) bond leads to a corresponding increase in the Fe–CN bond strength. While the difference in sensitivity to changes in the strength of the proximal bond between the linear and bent forms is expected, less expected is the predicted direct proportionality between the Fe–C–N vibrational frequency and the strength of the proximal Fe–N_ϵ(His). Owing to the predominance of σ-bonding between the iron and the

cyanide (Tanaka, 1987), both of the axial ligands compete for the d_{z^2} orbital of the iron. Therefore, stronger σ-bonding from the proximal Fe–N_ϵ(His) should be expected to weaken the Fe–CN bond. This argument is consistent with experimental observations for the cyanide adducts of model compounds, which indicate that strengthening of the trans-axial ligand bond weakens the Fe–C bond of the bound cyanide (Uno, 1988). Therefore, the observed 5-cm^{-1} downshift in the ν[Fe–CN] mode of the second conformer upon the acid–alkaline transition could be brought about by a stronger trans-proximal Fe–N_ϵ(His) bond, which could be induced through a conformational change in the protein structure or by a further increase in the imidazolate character of the proximal histidine. This argument is supported by the observed upshift in the Fe–N_ϵ(His) stretching frequency in the native ferric HRP upon the acid–alkaline transition (Teraoka, 1981).

The structural interpretation outlined above specifies a hydrogen-bonding interaction with Arg-38 as the source of the bent conformer. A reasonable alternative explanation is that the distal histidine might assume two distinct orientations, one of which would give rise to a bent conformer (Oldfield, 1991; Makinen, 1979; Maxwell, 1976). In fact, recent NMR experiments (Thanabal, 1988) which focused on the pH dependence of the exchangeable proton resonances of HRP–CN unambiguously demonstrated that the bound cyanide is hydrogen-bonded to the imidazolium group of the distal histidine. The chemical shifts of the heme peripheral methyl groups were found to be sensitive to the isotopic composition of the solvent, giving two distinct resonances in 1:1 H_2O/D_2O at low pH which collapse to one resonance at an intermediate position when the pH was raised to a value where the H/D exchange of the imidazolium proton is fast on the NMR time scale.

Nevertheless, the current interpretation is not inconsistent with the NMR data if it is assumed that the exchange rate of the arginine proton with bulk solvent is fast. In fact, this possibility is suggested on the basis of the fact that the exchangeable arginine proton is not observed in the NMR spectrum (although the lack of the observable resonance could also result from the fact that the arginine is believed to lie close to the magic angle and thus may not be resolved from the diamagnetic envelope). Thus, the observable shifts of the heme methyl groups, in both H_2O and D_2O, are a time average for the interaction with both the histidine and the arginine.

Although possible orientational disorder of the distal histidine cannot be ruled out as the source for the bent conformer, several considerations favor the proposed interaction with the arginine residue. First, the distal histidine is known to form a hydrogen bond between the $N_\delta H$ and the carbonyl fragment of Asn-82 which should stabilize its orientation (Edward, 1990). In fact, the NMR resonance corresponding to this exchangeable proton does not broaden significantly under conditions where the N_ϵ proton (involved with the hydrogen-bonding interaction with bound cyanide) does, implying a relatively stable configuration (Thanabal, 1988). Additionally, crystal structure data for the structurally analogous CCP–CN complex (Edward, 1990) show that the corresponding arginine residue lies 0.3 Å closer to the bound cyanide than it does to the bound CO in the structurally similar ferrous CO adduct, a fact which has been interpreted to indicate stronger interaction (presumably hydrogen bonding) with the cyanide.

(3) Comparison with the CO Adduct of Ferrous HRP. Spiro and co-workers (Evangelista-Kirkup, 1986) reported that CO binds to ferrous HRP to form two species, the relative population being dictated by the pH of the medium. The first species predominates at high pH and exhibits axial mode frequencies characteristic of a linear Fe–C–O linkage and a strongly hydrogen-bound proximal histidine. The second species predominates at low pH and exhibits axial mode frequencies characteristic of a tilted Fe–C–O linkage that is strongly hydrogen-bonded to a distal histidine. It is to be noted that a similar study carried out by Uno et al. (1987) also identified multiple species, although the two studies were not entirely consistent. Unlike the cyanide adducts of ferric HRP, which give rise to two H-bonded conformers, the CO-bound ferrous HRP apparently exists in only one conformer at a given pH, being tilted and hydrogen-bound to a protonated distal histidine (low pH) or linear and not hydrogen-bonded (high pH). As was mentioned above, the crystal structures of the CN^- and CO adducts of the biologically related cytochrome *c* peroxidase (Edwards, 1990) reveal that the arginine residue is 0.3 Å closer to the bound CN^- than it is to the bound CO, implying a lack of hydrogen bonding to the arginine in the case of CO. This difference in behavior between the CN^- and CO adducts of HRP is consistent with the known flexibility of the distal arginine residue and the enhanced strength of the hydrogen-bonding to negatively charged CN^- relative to bound CO. Therefore, the pH-dependent shifts observed for the CO adducts of ferrous HRP can be ascribed solely to the elimination of the H-bond with distal histidine.

Functional Implications. The active sites of all peroxidases contain a strongly hydrogen-bonded (imidazolate-like) proximal histidine and two or more distal-side proton donor/acceptor groups (e.g., His, Arg, Asp, Trp, ..., etc.) which are capable of interacting with the natural substrate, hydrogen peroxide. Thus, both the proximal- and the distal-side environments promote heterolytic cleavage of hydrogen peroxide as a result of the concerted influence of both factors: the so-called "push–pull" effect (Finzel, 1984; Poulos, 1987; Thanabal, 1988; Dawson, 1988; Traylor, 1990; Dunford, 1991; Yamaguchi, 1993). The present RR results provide clear evidence for the direct interaction of the exogenous ligands (in this case, CN^-) with both distal-side hydrogen bond donor groups. Furthermore, deprotonation of the distal-side histidine (which can be viewed as corresponding to proton transfer to the terminal oxygen atom of hydrogen peroxide during heterolytic cleavage) induces a change in the proximal histidine bonding to the heme iron. On the basis of our current understanding (Uno, 1988) of the electronic structure of the B–FeP–CN fragment (where B is the trans-axial ligand), a decrease in the ν[Fe–CN] stretching frequency implies an increase in the trans-axial ligand bond strength. Such an increase in the trans-proximal histidine bond strength has been shown to facilitate heterolytic O–O bond cleavage in a series of model compound studies (i.e., an increase in the "push effect") (Yamaguchi, 1993). The present RR study thus provides the first direct observation of a simultaneous increase in the "push" effect upon proton transfer from the distal histidine (i.e., the "pull" effect).

REFERENCES

Banci, L., Bertini, I., Turano, P., Ferrer, J. C., & Mauk, A. G. (1991) *Inorg. Chem. 30*, 4510–1516.

Behere, D. V., Gonzalez-Vergara, E., & Goff, H. M. (1985) *Biochim. Biophys. Acta 832*, 319–325.

Bhattacharyya, D. K., Bandyopadhyay, U., & Banerjee, R. K. (1992) *J. Biol. Chem. 267*, 9800–9804.

Caughey, W. S., Shimada, H., Choc, M. G., & Tucker, M. P. (1981) *Proc. Natl. Acad. Sci. U.S.A. 78*, 2903–2907.

Caughey, W. S., Shimada, H., Hazzard, J. H., Houtchens, R. A., Potter, W. T., & Einarsdottir, O. (1983) *Fed. Proc., Fed. Am. Soc. Exp. Biol. 42*, 2000.
Chance, B., Powers, L., Ching, Y., Poulos, T., Yamazaki, I., & Paul, K. J. (1984) *Arch. Biochem. Biophys. 235*, 596.
Dawson, J. H. (1988) *Science 240*, 433–439.
de Ropp, J. S., La Mar, G. N., Smith, K. M., & Langry, K. C. (1984) *J. Am. Chem. Soc. 106*, 4438–4444.
Dunford, H. P. (1982) *Adv. Inorg. Biochem. 4*, 41–68.
Dunford, H. P. (1991) *Peroxidases in Chemistry and Biology* (Everse, J., Everse, K. E., & Grisham, M. B., Eds.) Vol. II, pp 1–24, CRC Press, Boca Raton, FL.
Edwards, S. L., & Poulos, T. L. (1990) *J. Biol. Chem. 265*, 2588–2595.
Evangelista-Kirkup, R., Smulevich, G., & Spiro, T. G. (1986) *Biochemistry 25*, 4420–4425.
Finzel, B. C., Poulos, T. L., & Kraut, J. (1984) *J. Biol. Chem. 259*, 13027–13036.
Frauenfelder, H., Sligar, S. G., & Wolynes, P. G. (1991) *Science 25*, 1598–1603.
Han, S., Madden, J. F., Siegel, L. M., & Spiro, T. G. (1989) *Biochemistry 28*, 5477–5485.
Hu, S., Treat, R. W., & Kincaid, J. R. (1993) *Biochemistry* (in press).
La Mar, G. N., de Ropp, J. S., Smith, K. M., & Langry, K. C. (1980) *J. Biol. Chem. 255*, 237–243.
La Mar, G. N., Thanabal, V., Johnson, R. D., Smith, K. M., & Parish, D. W. (1989) *J. Biol. Chem. 264*, 5428–5434.
Lopez-Garriga, J. J., Oertling, W. A., Kean, R. T., Hoogland, H., Wever, R., & Babcock, G. T. (1990) *Biochemistry 29*, 9387–9395.
Makinen, M. W., Houtchens, R. A., & Caughey, W. S. (1979) *Proc. Natl. Acad. Sci. U.S.A. 76*, 6042–6046.
Maxwell, J. C., & Chaughey, W. S. (1976) *Biochemistry 15*, 388–396.
Morikis, D., & Champion, P. M. (1989) *Biochemistry 28*, 4791–4800.
Morishima, S. O., Ogawa, S., Inubushi, T., Yonezawa, T., & Iizuka, T. (1977) *Biochemistry 16*, 5109–5114.
Oldfield, E., Guo, K., Auguspurger, J. D., & Dykstra, C. E. (1991) *J. Am. Chem. Soc. 113*, 7537–7541.
Palmer, G. (1979) in *The Porphyrins* (Dolphin, D., Ed.) Vol. IV, pp 313–331, Academic Press, New York.
Poulos, T. T. (1987) *Adv. Inorg. Biochem. 7*, 1–36.
Sage, J. T., Li, P., & Champion, P. M. (1991a) *Biochemistry 30*, 1237–1247.
Sage, J. T., Morikis, D., & Champion, P. M. (1991b) *Biochemistry 30*, 1227–1237.
Sakurada, J., Takahashi, S., & Hosoya, T. (1986) *J. Biol. Chem. 261*, 9657–9662.
Shannon, L. M., Kay, E., & Lew, J. Y. (1966) *J. Biol. Chem. 241*, 2166–2172.
Sitter, A. J., Shifflett, J. R., & Turner, J. (1988) *J. Biol. Chem. 263*, 13032–13038.
Spiro, T. G., & Li, X.-Y. (1988) in *Biological Applications of Raman Spectroscopy* (Spiro, T. G., Ed.) pp 1–37, Wiley, New York.
Tanaka, T., Yu, N.-T., & Chang, C. K. (1987) *Biophys. J. 52*, 801–805.
Teraoka, J., & Kitagawa, T. (1981) *J. Biol. Chem. 256*, 3969–3977.
Thanabal, V., de Ropp, J. S., & La Mar, G. N. (1987) *J. Am. Chem. Soc. 109*, 7516–7525.
Thanabal, V., de Ropp, J. S., & La Mar, G. N. (1988) *J. Am. Chem. Soc. 110*, 3027–3035.
Traylor, T. G., & Xu, F. J. (1990) *J. Am. Chem. Soc. 112*, 178–186.
Uno, T., Nishimura, Y., Tsuboi, M., Makino, R., Iizuka, T., & Ishimura, Y. (1987) *J. Biol. Chem. 262*, 4549–4556.
Uno, T., Hatano, K., Nishimura, Y., & Arata, Y. (1988) *Inorg. Chem. 27*, 3215–3219.
Yamaguchi, K., Watanabe, Y., & Morishima, I. (1993) *J. Am. Chem. Soc. 115*, 4058–4065.
Yamazaki, I., Araiso, T., Hayashi, Y., Yamada, H., & Makino, R. (1978) *Adv. Biophys. 11*, 249–281.
Yoshikawa, S., O'Keeffe, D. H., & Caughey, W. S. (1985) *J. Biol. Chem. 260*, 3518–3528.
Yu, N.-T., & Kerr, E. A. (1988) in *Biological Application of Raman Spectroscopy* (Spiro, T. G., Ed.) pp 39–95, Wiley, New York.
Yu, N.-T., Benko, B., Kerr, E. A., & Gersonde, K. (1984) *Proc. Natl. Acad. Sci. U.S.A. 81*, 5106–5110.